

# Preliminary experimental analysis of a CdTe BIPV skylight on a lab-scale test cell

*Octavian-Gabriel Pop*<sup>1</sup>, *Elmakki Ali Elmakki Mustafa*<sup>2</sup>, *Mircea Lăcrăjan*<sup>3</sup> and *Lucian Fechete-Tutunaru*<sup>4\*</sup>,

<sup>1</sup>Technical University of Cluj-Napoca, Building Services Engineering Department, 40064 Cluj-Napoca, Romania

<sup>2</sup>Technical University of Cluj-Napoca, Mechanical Engineering Department, 400641 Cluj-Napoca, Romania

<sup>3</sup>Technical University of Cluj-Napoca, Electrical Engineering Department, 400027 Cluj-Napoca, Romania

<sup>4</sup>Technical University of Cluj-Napoca, Automotive Engineering and Transportation Department, 400641 Cluj-Napoca, Romania

**Abstract.** The recent goal of developing new solar energy-harvesting methods has led to the study and implementation of Building Integrated Photovoltaic (BIPV) glazing structures integrated into building envelopes. Thus, currently, the most energy-efficient substitute for traditional building glazing components is the BIPV window; however, to achieve a wide level of implementation, research is still required. This paper presents an experimental test chamber designed to investigate the effectiveness of a semi-transparent BIPV glazing skylight with a 40% degree of transparency. Weather parameters were monitored using a laboratory-manufactured weather station. At its peak, the PV power output is 36.78 W, at a global solar irradiance of 573.69 W/m<sup>2</sup>. Values of 67.25 °C were displayed by temperature sensors mounted on the outer glazing surface. The air temperature reached high values near the globe thermometer signals because of the small test cell size and thermal insulation. The interior illuminance values during the operation stabilised at ~16.6 klx. The experimental data were compared with findings from related research. The ranges of the results obtained in the current study matched those of previous research.

## 1 Introduction

As efficient harvesting of solar energy is an important goal in building engineering, Building Integrated Photovoltaic (BIPV) systems have become popular, taking advantage of constructed building façades and roof surfaces to generate photovoltaic (PV) power [1]. Therefore, the use of semi-transparent PV glazing surfaces has attracted the attention of many researchers in the field [2]. Moreover, a review study by Mohammad et al [3] recommends that further research should be conducted on PV windows, considering that these types of glazing systems are the most efficient alternatives to classic window units of buildings,

---

\* Corresponding author: [Lucian.Fechete@auto.utcluj.ro](mailto:Lucian.Fechete@auto.utcluj.ro)

due to their capacity to incorporate the function of daylight harvesting as well as the extra feature of producing PV energy [4]. BIPV glazing units are categorized based on the type of PV element integrated into the module, such as amorphous silicon thin films, crystalline solar cells, polycrystalline solar cells, Cadmium Telluride (CdTe) thin films etc. [4], [5].

An experimental investigation of different configurations of vertically mounted vacuum-glazing units equipped with CdTe film was conducted by Huang et al. [6]. The impact of the application of low-E coating was studied.

In Uddin et al. [7], a test cell with vertically mounted south-facing CdTe glazing units with an 80% cell coverage ratio was employed to investigate the performance of PV windows under summer climatic conditions. The test indicated that the exterior window surface temperature could peak slightly above 50 °C, and the maximum interior room temperature was approximately 34 °C. Electrical power generation can reach a maximum of ~30 W, and indoor lighting levels reach peak values close to 400 lx.

Wu et al. [8] studied a single-glazing window equipped with monocrystalline silicon PV cells with a cell coverage of 55%. The unit was mounted vertically and south-oriented. The experiment was conducted under exterior conditions with maximum global solar irradiance values between 400-500 W/m<sup>2</sup>. The peak power output was slightly above 60 W, and the surface temperature of the PV cell reached values above 40 °C.

Concentrating Photovoltaic modules were implemented in a prototype proposed by Ghoraishi et al. [9], equipped with a ventilated layer for heat recovery. Experiments were performed under laboratory conditions to validate numerical simulation methods. The solution was then numerically investigated, revealing that the power output could range from 63.32 to 92.56 W/m<sup>2</sup>.

A PV window with an integrated vacuum layer that serves a full-scale experimental room was investigated by Tan et al. [10] and employed to validate a multi-physics model. The study concluded that a 40% PV coverage should be considered for the optimal design of PV windows.

Wang et al. [11] employed an experimental method to compare the efficiency of different BIPV window configurations with classic solutions. High temperature differences between the external and internal surfaces of the unit were observed when the radiative-cooling coating was applied. The indicated difference was 22.22 °C almost twice as high as that of the PV window version without coating.

The coupling of vacuum-enhanced monocrystalline PV windows and thermoelectric elements was studied by Yang et al. [12]. The PV cells cover 60% of the glazing elements. The module's thermal performance is studied, and it is concluded that the system produces a temperature decrease of 9.6 °C and an increase of 6.2 °C during summer and winter, respectively.

This paper presents an experimental study conducted on a BIPV skylight tilted at an angle of 30° using a CdTe film for solar harvesting. The experimental rig consisted of a test chamber that monitored the external and internal temperatures measured by two arrays of digital sensors mounted on the glass surfaces. Interior parameters such as air temperature and lighting level were measured and studied.

Weather parameters were monitored using a laboratory-manufactured local weather station, located near the experimentation site.

## 2 Experimental methodology

An experimental test cell manufactured out of plasterboard exterior sandwich walls with polystyrene thermal insulation and designed to test a semi-transparent BIPV skylight system was employed in the current study. A 1200 × 600 mm triple-glazing unit was tested. The unit consisted of an external 7 mm thick CdTe glazing element with a transparency of 40%, two

4 mm glass layers, and external and internal air layers with thicknesses of 12 and 8 mm, respectively. The term “transparency” refers to the area of the PV glass surface that permits light transmission. Therefore, a transparency of 0% indicates that the glass is completely opaque and 100% indicates full transparency. Transparency is an important characteristic to factor into PV glass selection, as it plays a significant role in windows’ PV power output, as well as the possibility of ensuring daylighting.

The experiment was conducted in Cluj-Napoca, Faculty of Building Services Engineering, Technical University of Cluj-Napoca, Romania, as illustrated in Fig. 1.

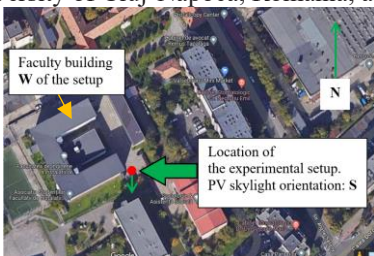


**Fig. 1** Experimentation site.

Fig. 2 shows the experimental rig at the testing site. The rig was equipped with 2×9 DS18B20 digital temperature sensors mounted on the outer (o) and inner (i) surfaces of the skylight unit. A DAV 6450 solar radiation sensor was mounted next to the skylight at a 30° tilt angle to measure the global solar irradiance ( $I_{gl}$  [ $W/m^2$ ]) with a spectral response of (400-1100) nm, covering the spectral response range of the CdTe thin film that is situated within ~ (400-900) nm [13]. An identical solar radiation sensor was mounted within a shadow ring for diffuse solar irradiance measurements ( $I_{dif}$  [ $W/m^2$ ]). A lux probe was placed in front of the cell to measure the natural light level ( $E_{v,ext}$  [lx]).

Within the test cell, at the centre of the chamber floor, a shaded DS18B20 digital temperature sensor for air temperature measurements was placed ( $T_{a,int}$  [°C]) and a Globe Thermometer Ø 150 mm equipped with a Type K thermocouple (GT [°C]). A TESTO lux probe to assess the level of lighting within the interior ( $E_{v,int}$  [lx]) was also added.

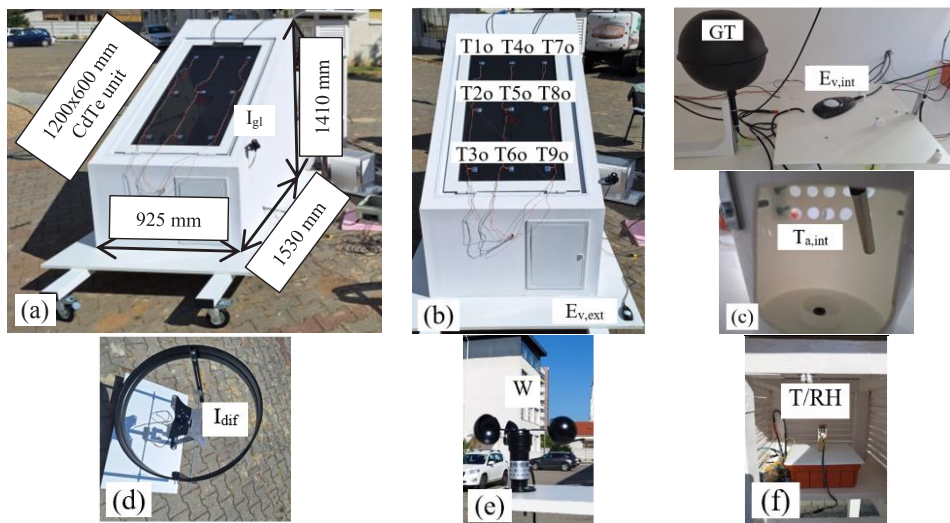


**Fig. 2** Experimental rig (a) Exterior view, (b) outer PV glass temperature sensor network (c) interior view, (d) solar radiation sensor in shadow ring, (e) weather station anemometer, and (f) weather station interior.

An identical network of sensors was mounted on the internal surface of the skylight, considering the same numbering system, and position, further noted with the index “i”.

The interior air temperature was measured by a digital sensor protected from solar radiation, within a small white interior cell that also allows circulation of surrounding air as indicated in international standard ISO 7243 [14] and shown in Fig. 2c. Based on the globe thermometer readings, the mean radiant temperature (MRT), noted as  $\bar{T}_r$  [°C], was estimated. The MRT is approximated using the method given in ISO 7726 [15] factoring in the convection effect produced by the surrounding air. Due to the small dimensions of the test cell and the absence of any mechanical ventilation within the chamber, the MRT was estimated considering natural convection occurring between the globe and the interior air, using the following equation [15]:

$$\bar{T}_r = \left[ (T_g + 273.15)^4 + \frac{0.25 \cdot 10^8}{\epsilon_g} \cdot \left( \frac{T_g - T_{a,int}}{D} \right)^{0.25} \cdot (T_g - T_{a,int}) \right]^{0.25} - 273.15 \quad (1)$$

where  $T_g$  [°C] is the globe temperature considered equal to  $GT$  [°C] according to [14], [15],  $\epsilon_g=0.95$  [-] is the emissivity of the globe (matt black paint) and  $D=0.15$  m is the diameter of the globe. The employed globe thermometer is in compliance with standard ISO 7243.

Aside from the level of solar radiation and daylight, which were monitored with equipment attached to the test rig, a laboratory-manufactured weather station was placed in the vicinity of the rig to measure the exterior air parameters. The analytical breakdown of the measuring equipment is presented in Table 1.

**Table 1.** Characteristics of the equipment

Notation	Characteristics
T	Temperature sensor DS18B20, Type: Digital, Range: -55÷ +125 °C, Accuracy: ±0.5 °C
Ev	Lux probe, Type: Digital, Range: 0÷100000 lux, Accuracy: F1 = 6 % = V(Lambda) adjustment; F2 = 5% cos-like weighting (in compliance with DIN EN 13032-1 and class C according to DIN 5032-7)
GT	Globe thermometer, Ø 150mm, Type K thermocouple, Type: Digital, Range: 0÷ 120 °C, Accuracy Class 1 (in compliance with ISO 7243 and ISO 7726)
I	Solar Radiation Sensor DAV-6450, Type: Analog, Range: 0÷1800 W/m <sup>2</sup> , Sensitivity: 1.67 mV per W/m <sup>2</sup> , Accuracy: ±5%, Spectral Response (10% points): 400-1100 nm (same as CdTe film)
T/RH	Temperature and humidity sensor SEN0334, Type: Digital, Range: -40°C÷125°C/0÷100%, Accuracy: ±0.2°C/±2%
W	Three-cup anemometer, Type: Analog, Range: 0÷30 m/s, Accuracy: ±3%

An Arduino UNO board processes the digital and analogue inputs from the temperature sensors, mounted on the glazing surfaces, and from the solar radiation sensor, respectively.

A voltage divider with two resistors having electrical resistances of 120 Ω and 5 Ω, respectively, was used as a load for PV power output ( $P_{PV}$  [W]) measurements and to convert the measured values within the Arduino UNO input range.

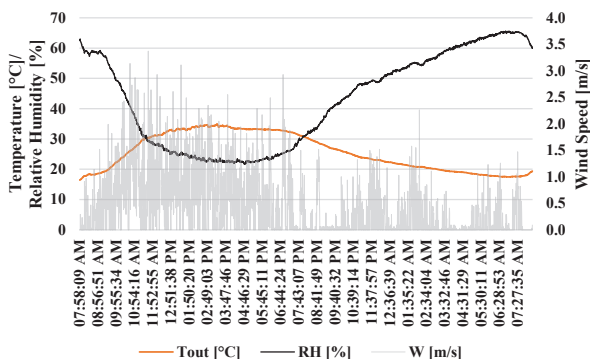
The Arduino UNO was powered by a laptop behind the test cell, which also received and stored data at 30s intervals.

The lux probes and globe thermometer are connected to a Testo IAQ Data Logger that receives data at 5-minute intervals. The Data Logger was programmed using a Testo 400 Universal device, which also saved the measurements stored by the Data Logger, at the end of the measuring period, and transferred them to the laptop for further processing using the Testo DataControl software.

### 3 Results and Discussion

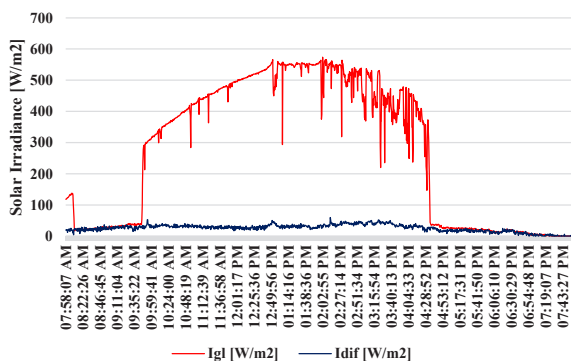
#### 3.1 Weather parameters

The experiment was conducted on August 25, 2024. The outdoor air temperature, relative humidity, and wind speed are shown in Fig. 3. A hot period was selected for the experimental study. The outdoor air is characterised by high temperatures, reaching a maximum of 34.87 °C, at 03:20 PM, and low relative humidity.



**Fig. 3** The weather parameters during a 24h period, between 25-26.08.2024.

The global solar irradiance was measured on the surface tilted at 30° and presented in Fig. 4, for the 12h period of the experiment, from approximately 08:00 AM to 08.00 PM.



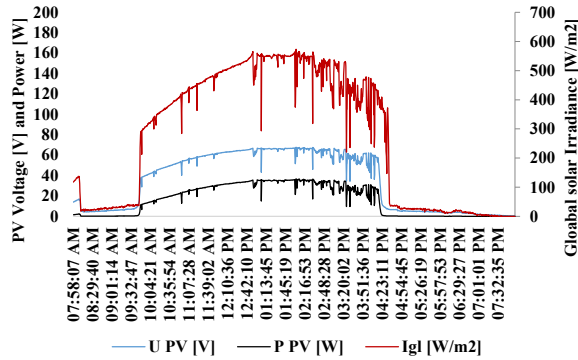
**Fig. 4** Global solar irradiance on a 30° tilted surface.

Fig. 4 shows the time interval when solar radiation was available for PV power generation.

#### 3.2 PV power and glass temperature measurements

##### 3.2.1 Generated PV power

Fig. 5 shows the PV power generated by the CdTe element. Before noon, very little cloud coverage was present, compared to the afternoon, when variations and drops in solar radiation intensity could be observed.



**Fig. 5** Voltage and PV power generated by the CdTe glazing unit, and the global solar irradiance on the tilted surface of the skylight.

The PV power output peaked at 36.78 W, at 02:02 PM, when the sensor indicated a global solar irradiance of 573.69 W/m<sup>2</sup>. The voltage measured at this time was 67.8 V.

In the afternoon, the PV power output dropped before the global solar radiation sensor readings indicated that solar energy was no longer available. This is because the CdTe glass panel is partially shaded by the building west of the cell, while the global solar radiation sensor is still exposed to the sun for an extra 17 min.

### 3.2.2 Variation of measured temperatures

To assess the effect of the skylight on the interior environment of the cell, the temperatures measured by the sensors mounted on the external and internal glass surfaces are presented in Fig. 6, as measured by the column of sensors: T<sub>4o</sub>, T<sub>5o</sub>, T<sub>6o</sub>, T<sub>4i</sub>, T<sub>5i</sub>, and T<sub>6i</sub>.

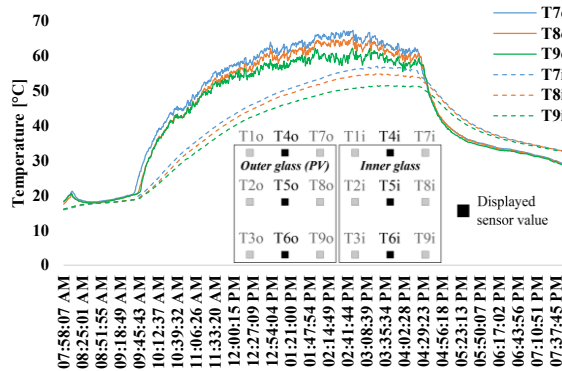


**Fig. 6** Temperatures measured by the sensors mounted in positions 4, 5, and 6, on the outer (o) and inner (i) skylight surface.

Between 12:33 PM and 04:19 PM, the temperature sensors on the outer surface indicated values above 65 °C because of the prolonged exposure of the glass surface to the sun.

Within the test cell, the globe thermometer readings, air temperature and estimated mean radiant temperature are presented in Fig. 7 for analysis.

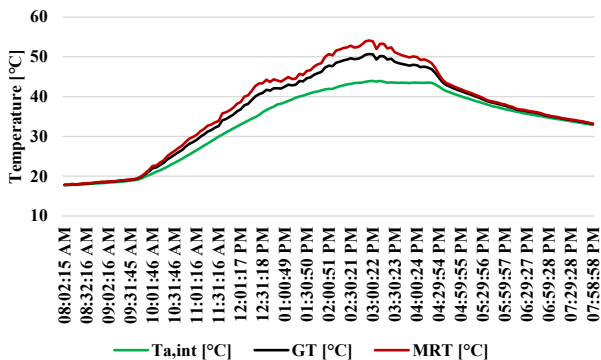


**Fig. 7** Measured temperatures within the test cell.

As can be observed, due to the thermal insulation of the exterior opaque elements, the high exterior temperatures, transmitted solar radiation and the small dimensions of the cell, the interior air and mean radiant temperatures reach high values.

### 3.2.3 Level of lighting

During the operation period, the level of exterior lighting was high, reaching values of approximately 90 klx. The lighting level within the setup was relatively stable at ~ 16.6 klx, between 12:19 PM and 03:09 PM. During 09:00 AM and 05:00 PM, the skylight glazing structure led to a reduction of 86.52% of the natural lighting level. Fig. 8 shows the variations in the exterior and interior lighting levels during the operation of the test rig.

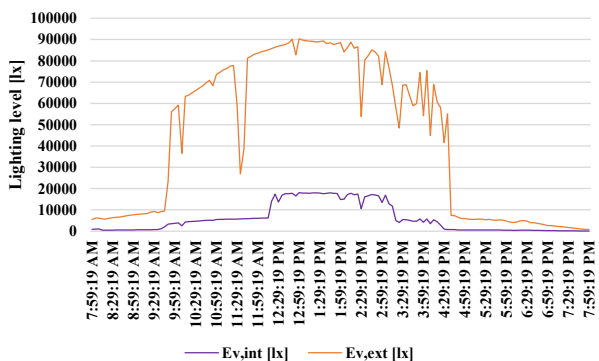


**Fig. 8** Level of interior and exterior luminous flux during the experiment

### 3.2.4 Results analysis and discussions of the PV performance

The experimental results presented in this study were compared with those of similar studies in the literature. The comparison is presented in Table 2.

**Table 2.** Comparison of current and similar studies.

PV element	Mono-crystalline PV cells	CdTe		
Mounting	V	V	V	*30°
P <sub>PV,max</sub>	65.7 W	~30 W	-	36.78 W
Size	1644×986×8 mm	1100×600×3 mm	300×200 mm	1200×600×7 mm
T <sub>o,max</sub>	-	>50 °C	-	67.25 °C
T <sub>i,max</sub>	PV cell/Glass ~42.5/37.5 °C	~40 °C	39.10 – 54.83 °C	56.94 °C
T <sub>a,int,max</sub>	-	~34 °C	48.82- 33.20 °C	44 °C
E <sub>v,int</sub>	-	~400 lx	1.6-25.0 klx	~16.6 klx
Ref.	[8]	[7]	[16]	<i>This study</i>

\*Tilt angle.

The results of the current study and those presented in [7] were obtained in similar periods of the year, July and August, respectively, employing similar PV properties of the investigated model, thus, resulting in similar power output. Also, the outer temperature measured values at the surface level of the PV were similar. In very similar meteorological conditions as the present work, Wu et al. [8] investigated the performance of monocrystalline cells integrated in a semi-transparent glazing unit, resulting in approximately double the power output compared to the CdTe film. Monocrystalline cells are known to produce significantly higher amounts of electrical energy than CdTe elements, thus explaining the difference. Also, the model presented in [8] operated at lower temperatures, such as inner temperatures measured at the surface of the glazing unit of T<sub>i</sub>=40 °C, compared to T<sub>i</sub>=56.94 °C as measured in the present study. Moreover, the efficiency of monocrystalline cells is more sensitive to temperature variations, being characterized by a power temperature coefficient of -0.36÷-0.38 %/K [17], [18], while the CdTe film has a temperature coefficient of -0.214 %/K [19]. Shi et al. [16] experimentally investigated the influence of CdTe PV widows on the thermal environment and lighting performance within a test cell. The parameters measured in this study are in agreement with the values presented in [16]. Shi et al. [16] conducted a simulation study to assess the impact of PV energy production, relative to the energy consumption of the studied building.

## 4 Conclusions

This paper presents an experimental test cell manufactured to analyse the operation of a PV skylight system for buildings. An overview of the equipment used to measure the studied parameters was presented.

A weather station was used simultaneously with the experimental trial to assess the exterior conditions of operation. Solar radiation as well as the exterior level of natural lighting were also monitored.

The parameters of interest of the test cell were PV power output, temperatures measured with sensors mounted on the inner and outer glazing surfaces, interior temperatures measured with a globe thermometer and a shaded digital sensor, and interior lighting level.

The PV power output reached a peak value of 36.78 W ( $I_{gl}=573.69 \text{ W/m}^2$ ).

The temperature sensor mounted on the outer glazing surface exhibited values of maximum 67.25 °C.

The variation of interior temperatures is also presented; the air temperature reaches high values, relatively close to the globe thermometer indications, due to the small size of the test cell and thermal insulation.

The interior lighting levels were 86.52% lower than the outdoor environment and stabilised at ~16.6 klx during the afternoon.

The experimental data were compared with results from similar studies. Thus, certain deductions can be made regarding the advantages and disadvantages of the implementation of such skylight systems. The studied module has generated comparable PV power to a similar system. However, in comparison to PV power generation resulting from employing monocrystalline cells in windows, the power output of the current study is naturally lower, thus the analysis of different PV solutions in windows is essential.

Further research is required to achieve better PV performance from both electrical and thermal perspectives. Methods for cooling PV glazing for better power generation efficiency and higher interior thermal comfort represent future research directions. The implementation of phase change materials and heat recovery systems will represent future research topics of the authors.

**Acknowledgement:** This study was supported by the Technical University of Cluj-Napoca, a member of the Romanian Alliance of Technical Universities (ARUT), through the GNaC ARUT 2023 research grants program, in the framework of the project UNIVERSAL "The impact of PV-glazed façades with PCM cooling on the HVAC systems of buildings" Contract No. 21/01-07-2024.

## References

1. L. Chen, Y. Sun, N. Zhang, J. Yang, and D. Wang, "Quantifying the benefits of BIPV windows in urban environment under climate change: A comparison of three Chinese cities," *Renew Energy*, vol. 221, Feb. 2024, doi: 10.1016/j.renene.2023.119740.
2. M. M. Uddin, J. Jie, C. Wang, C. Zhang, and W. Ke, "A review on photovoltaic combined vacuum glazing: Recent advancement and prospects," May 01, 2023, *Elsevier Ltd.* doi: 10.1016/j.enbuild.2023.112939.
3. A. K. Mohammad, A. Garrod, and A. Ghosh, "Do Building Integrated Photovoltaic (BIPV) windows propose a promising solution for the transition toward zero energy buildings? A review," Nov. 15, 2023, *Elsevier Ltd.* doi: 10.1016/j.jobe.2023.107950.
4. Y. Sun *et al.*, "Integrated semi-transparent cadmium telluride photovoltaic glazing into windows: Energy and daylight performance for different architecture designs," *Appl Energy*, vol. 231, pp. 972–984, Dec. 2018, doi: 10.1016/j.apenergy.2018.09.133.
5. H. Musameh, H. Alrashidi, F. Al-Neami, and W. Issa, "Energy performance analytical review of semi-transparent photovoltaics glazing in the United Kingdom," Aug. 15, 2022, *Elsevier Ltd.* doi: 10.1016/j.jobe.2022.104686.
6. J. Huang, Q. Wang, X. Chen, S. Xu, and H. Yang, "Experimental investigation and annual overall performance comparison of different photovoltaic vacuum glazings," *Sustain Cities Soc*, vol. 75, Dec. 2021, doi: 10.1016/j.scs.2021.103282.
7. M. M. Uddin, C. Wang, C. Zhang, and J. Ji, "Investigating the energy-saving performance of a CdTe-based semi-transparent photovoltaic combined hybrid

- vacuum glazing window system,” *Energy*, vol. 253, Aug. 2022, doi: 10.1016/j.energy.2022.124019.
8. Z. Wu, L. Zhang, J. Wu, and Z. Liu, “Experimental and numerical study on the annual performance of semi-transparent photovoltaic glazing in different climate zones,” *Energy*, vol. 240, Feb. 2022, doi: 10.1016/j.energy.2021.122473.
  9. M. Ghorraishi, T. Hyde, A. Zacharopoulos, J. D. Mondol, and A. Pugsley, “Concentrating Photovoltaic/Thermal Evacuated Glazing (CoPVTEG); Introduction and computational analysis,” *Solar Energy*, vol. 263, Oct. 2023, doi: 10.1016/j.solener.2023.111814.
  10. Y. Tan *et al.*, “Daylight-electrical-thermal coupling model for real-time zero-energy potential analysis of vacuum-photovoltaic glazing,” *Renew Energy*, vol. 205, pp. 1040–1056, Mar. 2023, doi: 10.1016/j.renene.2023.01.116.
  11. W. Wang, H. Yang, and C. Xiang, “The overall performance of a novel semi-transparent photovoltaic window with passive radiative cooling coating – A comparative study,” *Energy Build*, vol. 317, Aug. 2024, doi: 10.1016/j.enbuild.2024.114433.
  12. J. Yang *et al.*, “A novel vacuum-photovoltaic glazing integrated thermoelectric cooler/warmer for environmental adaptation: thermal performance modelling,” *Renew Energy*, vol. 229, Aug. 2024, doi: 10.1016/j.renene.2024.120733.
  13. A. S. A. C. Diniz, T. P. Duarte, S. A. C. Costa, D. S. Braga, V. C. Santana, and L. L. Kazmerski, “Soiling Spectral and Module Temperature Effects: Comparisons of Competing Operating Parameters for Four Commercial PV Module Technologies,” *Energies (Basel)*, vol. 15, no. 15, Aug. 2022, doi: 10.3390/en15155415.
  14. *ISO 7243:2017 Ergonomics of the thermal environment — Assessment of heat stress using the WBGT (wet bulb globe temperature) index.*
  15. *ISO 7726:1998 Ergonomics of the thermal environment — Instruments for measuring physical quantities.*
  16. S. Shi, N. Zhu, Y. Li, and Y. Song, “Photo-thermal decoupling CdTe PV windows with selectively near-infrared absorbing ATO nanofluids,” *Renew Energy*, vol. 235, Nov. 2024, doi: 10.1016/j.renene.2024.121178.
  17. B. R. Paudyal and A. G. Imenes, “Investigation of temperature coefficients of PV modules through field measured data,” *Solar Energy*, vol. 224, pp. 425–439, Aug. 2021, doi: 10.1016/j.solener.2021.06.013.
  18. “[https://www.ertex-solar.at/.](https://www.ertex-solar.at/)”
  19. “[https://photovoltaicwindows.eu/.](https://photovoltaicwindows.eu/)”